Peroxynitrite-Mediated Nitration of the Stable Free Radical Tyrosine Residue of the Ribonucleotide Reductase Small Subunit †

ARTICLE *in* BIOCHEMISTRY · MAY 2000

Impact Factor: 3.02 · DOI: 10.1021/bi992206m · Source: PubMed

7 AUTHORS, INCLUDING:

Laurent Serani
Institut National de Physique Nucléaire et de …
70 PUBLICATIONS **696** CITATIONS
SEE PROFILE

Olivier Laprévote
Université René Descartes - Paris 5
245 PUBLICATIONS **4,184** CITATIONS
SEE PROFILE

Michel Lepoivre
Université Paris-Sud 11
73 PUBLICATIONS **3,050** CITATIONS
SEE PROFILE

Peroxynitrite-Mediated Nitration of the Stable Free Radical Tyrosine Residue of the Ribonucleotide Reductase Small Subunit†

Olivier Guittet,‡ Paulette Decottignies,§ Laurent Serani,|| Yann Henry,⊥ Pierre Le Maréchal,§ Olivier Laprévote,|| and Michel Lepoivre*,‡

Unité 8619, Centre National de la Recherche Scientifique, Université Paris-Sud, Orsay, France, Institut de Biotechnologie des Plantes, Université Paris-Sud, Orsay, France, Unité 350, Institut National de la Santé et de la Recherche Médicale, Institut Curie, Orsay, France, and Institut de Chimie des Substances Naturelles, Centre National de la Recherche Scientifique, Gif-sur-Yvette, France

Received September 22, 1999; Revised Manuscript Received January 31, 2000

ABSTRACT: Ribonucleotide reductase activity is rate-limiting for DNA synthesis, and inhibition of this enzyme supports cytostatic antitumor effects of inducible NO synthase. The small R2 subunit of class I ribonucleotide reductases contains a stable free radical tyrosine residue required for activity. This radical is destroyed by peroxynitrite, which also inactivates the protein and induces nitration of tyrosine residues. In this report, nitrated residues in the *E. coli* R2 protein were identified by UV−visible spectroscopy, mass spectrometry (ESI-MS), and tryptic peptide sequencing. Mass analysis allowed the detection of protein R2 as a native dimer with two iron clusters per subunit. The measured mass was 87 032 Da, compared to a calculated value of 87 028 Da. Peroxynitrite treatment preserved the non-heme iron center and the dimeric form of the protein. A mean of two nitrotyrosines per *E. coli* protein R2 dimer were obtained at 400 μM peroxynitrite. Only 3 out of the 16 tyrosines were nitrated, including the free radical Tyr122. Despite its radical state, that should favor nitration, the buried Tyr122 was not nitrated with a high yield, probably owing to its restricted accessibility. Dose−response curves for Tyr122 nitration and loss of the free radical were superimposed. However, protein R2 inactivation was higher than nitration of Tyr122, suggesting that nitration of the nonconserved Tyr62 and Tyr289 might be also of importance for peroxynitrite-mediated inhibition of *E. coli* protein R2.

Nitration of tyrosine amino acids by chemical reagents has been used in the past to obtain structural and functional information on the role of these residues in proteins. Recently, posttranslational modification of proteins by nitration has also been shown to be carried out by several biological reactive species, especially peroxynitrite[1] (*1*−*3*). Peroxynitrite is produced by the very fast reaction of two radical species, NO and the superoxide anion $O_2^{\bullet -}$ ($k = 6.7 \times 10^9$ $M^{-1}\cdot s^{-1}$) (*1*). It is a potent oxidant and a nitrating agent of short half-life (*4*). The reactivity of peroxynitrite with proteins includes oxidation of aromatic and sulfur-containing amino acids, nitration of tyrosine residues, and protein fragmentation (*5*−*7*). Tyrosine nitration induced by peroxynitrite has been reported in a dozen isolated proteins, in particular bovine Cu,Zn- and human Mn-superoxide dismutases (*8*, *9*), mouse neurofilament-L (*10*), and rat cytochrome P450 2B1 (*11*). As already observed (*10*), there is an obvious specificity in the nitration reaction, since in all these proteins only one or a few among all tyrosine residues reacted with peroxynitrite. Until now the molecular basis for such a selectivity has not been clearly understood.

Ribonucleotide reductase is a unique enzyme necessary for DNA synthesis and repair, catalyzing the reduction of ribonucleotides into the corresponding deoxyribonucleotides. In eukaryotes and *E. coli*, the structure is that of an $\alpha_2\beta_2$ complex, the small homodimeric β_2 (R2) subunit harboring a tyrosyl free radical close to an Fe−O−Fe diferric iron center. The large dimer (R1) carries redox-active cysteines at the active site and allosteric effector binding sites. Both the radical/metal center in R2 and the cysteines in R1 are required for activity (*12*). Rapidly proliferating cells such as tumor cells have a pronounced demand of deoxyribonucleotides for DNA replication and, therefore, are particularly dependent on ribonucleotide reductase activity for cell growth. In some reports on human or murine cancers, an elevated expression of NO synthase II (iNOS) has been found in the tumor tissue, for instance in infiltrating macrophages, suggesting that *in vivo*, tumor cells could have to endure a chronic exposure to nitrogen oxides (*13*−*16*). Ribonucleotide reductase is inhibited by the high-output macrophage iNOS activity, and this inhibition was demonstrated in cellular

† This work was supported by l'Association pour la Recherche contre le Cancer (Grant 9426) and by a SIDACTION grant from La Fondation pour la Recherche Médicale.

* Corresponding author: UMR 8619 CNRS, Bât. 430, UPS Orsay, F-91405 Orsay Cedex, France. Telephone: (33) 1 6915-7972. Fax: (33) 1 6985-3715. E-mail: michel.lepoivre@bbmpc.u-psud.fr.

‡ Centre National de la Recherche Scientifique, Université Paris-Sud.

§ Institut de Biotechnologie des Plantes, Université Paris-Sud.

|| Institut de Chimie des Substances Naturelles, Centre National de la Recherche Scientifique.

⊥ Institut National de la Santé et de la Recherche Médicale, Institut Curie.

[1] Peroxynitrite here refers to the different reactive species $ONOO^-$, ONOOH, and $ONOOCO_2^-$, the adduct of $ONOO^-$ with CO_2. "ONOOH" also includes the activated (ONOOH*) and/or caged radical [$^{\bullet}CO_2$, $^{\bullet}NO_2$] reactive forms which are produced from ONOOH.

10.1021/bi992206m CCC: $19.00
Published on Web 03/28/2000

models to support a major part of the antiproliferative activity of activated macrophages against tumor cells (*17*−*19*). In previous reports, we have shown that ribonucleotide reductase was reversibly inhibited by NO and irreversibly inactivated by peroxynitrite (*19*−*21*). The inhibitory mechanism of ribonucleotide reductase by NO is complex, involving in a first step a coupling reaction between NO and the tyrosyl free radical on the R2 protein, and, for the mouse protein which is the prototype of mammalian R2 proteins, the subsequent release of the diferric center (*21*). Inactivation by *S*-nitrosation of cysteines in a bacterial R1 subunit, probably including those at the active site, has been also described (*20*). Peroxynitrite effects on ribonucleotide reductase are less documented. At the level of protein R2, tyrosine nitration, free radical destruction, and protein inactivation have been demonstrated, but the relationship between nitration and the two other events is not clear (*21*). It has been reported that irreversible inactivation of *E. coli* protein R2 by the superoxide radical $O_2^{\bullet -}$ is also associated with the destruction of the tyrosyl radical and chemical modification of tyrosyl residues (oxidation in this case). However, the catalytically competent Tyr122 carrying the free radical was not modified, suggesting that inhibition of protein R2 and loss of the tyrosyl radical may happen following long-range electron transfer from aromatic residues on the protein surface to Tyr122 (*22*). It was thus important to determine whether peroxynitrite-induced nitration might include Tyr122 and to what extent inactivation of protein R2 might depend on the nitration of this critical residue.

In the present study, electrospray mass spectrometry (ESI-MS) and peptide sequencing were used to analyze tyrosine nitration in protein R2 from *E. coli*. Only 3 out of 16 tyrosine residues were consistently nitrated, including Tyr122. To our knowledge, this is the first evidence of an irreversible modification of the free radical tyrosine residue by a ribonucleotide reductase inhibitor. As ESI-MS is a method gentle enough for monitoring noncovalent interactions in proteins, we could also establish that the quaternary structure of the dimeric, iron-containing R2 protein (M_r = 87 028) was not altered after peroxynitrite treatment.

EXPERIMENTAL PROCEDURES

Proteins. The small R2 subunit of ribonucleotide reductase was overexpressed after transfection of *E. coli* bacteria, strain BL21(DE3)pLys S, with the plasmid pVNR2 encoding the *nrdB* gene of *E. coli* R2 (*23*), generously donated by Pr. M. Fontecave (DBMS−CEA, Grenoble, France). Protein R2 synthesis was induced by IPTG. The recombinant protein was purified essentially by ammonium sulfate precipitation and anion exchange chromatography using a DEAE DE52 (Whatman) column, as in ref *24*. The purified protein, at least 95% pure by SDS−PAGE, was stored in liquid N_2 in 50 mM Tris·HCl, pH 7.6, containing 10% glycerol. Protein R1 from *E. coli* was also a kind gift of Pr. M. Fontecave. Thioredoxin from *E. coli* was given by M. Miginiac-Maslow (IBP, Université Paris-Sud, France). Thioredoxin reductase was purchased from IMCO Corp. (SE-100 31 Stockholm, Sweden) and desalted on a P-6 acrylamide column (BioRad) immediately before use.

Peroxynitrite Treatment of E. coli Protein R2. Peroxynitrite was synthesized from nitrite and hydrogen peroxide, as described in ref *21*. The concentration of the solution was determined at 302 nm using a molar extinction coefficient of 1670 $M^{-1}\cdot cm^{-1}$ (*25*). Two hundred microliters of protein R2 5 μM in 50 mM Tris·HCl buffer, pH 7.6, was treated with 100−400 μM peroxynitrite at room temperature for 10 min. In reverse-order experiments, $ONOO^-$ was added to buffer alone, before addition of protein R2. All other steps were carried out at 4 °C. The protein sample was desalted first on a G-25 Sephadex column (Pharmacia) equilibrated in water, and fractions containing the protein were pooled. Ammonium acetate, pH 6, was added to a final concentration of 100 mM in order to displace phosphate ions that could be bound to the protein. After 15 min, the sample was desalted again on a G-25 Sephadex column equilibrated with water. The protein fractions were pooled again, concentrated to a volume less than 100 μL by ultrafiltration through a Centricon-30 membrane (Amicon Inc.), and finally desalted with a Bio-Gel P-6 polyacrylamide gel. The resulting sample in water was analyzed by UV−Vis spectroscopy for tyrosyl free radical content and protein nitrotyrosine formation, before storage at −80 °C.

Spectrophotometric Detection and Quantification of Nitrotyrosine in Protein R2. Absorption spectra of protein R2 in water (pH 5.5), or diluted in 50 mM NH_4HCO_3, pH 8.3, were recorded from 250 to 700 nm on a Uvikon 943 spectrophotometer. The concentration of protein R2 (dimer) was calculated using a molar extinction coefficient of 117 000 $M^{-1}\cdot cm^{-1}$ at 280 nm (*24*). The amount of nitrotyrosine was calculated at 425 nm and pH 8.3, using a calculated molar extinction coefficient of 4380 $M^{-1}\cdot cm^{-1}$ for authentic 3-nitrotyrosine, which agreed with that found for nitrotyrosine in BSA at pH 11.5 (*5*, *26*).

Tryptic Digestion, Separation, and Sequencing of Proteolytic Peptides. From 0.5 to 1 mg of protein R2 was digested in 0.1 M NH_4HCO_3, pH 8.3, with sequence-grade trypsin (Sigma) for 7 h at 37 °C, at a protease:protein ratio of 1:50 (w/w). The peptides were separated by reverse-phase HPLC, on a 0.46 cm × 15 cm Vydac C4 (300 Å) column. Peptides were eluted with a linear gradient from 0 to 70% acetonitrile in 0.1% trifluoroacetic acid, over 90 min, at a flow rate of 1 $mL\cdot min^{-1}$. Absorbance was recorded at 215 and 350 nm. Peptides absorbing at 350 nm were collected and further purified by reverse-phase HPLC, on a 0.46 cm × 25 cm Vydac C18 (90 Å) column. The extinction coefficient of nitrotyrosine did not vary along the elution gradient. Sequencing was performed using an Applied Biosystems Model 476 A sequencer equipped with an on-line analyzer of phenylthiohydantoin amino acids.

Mass Spectrometry Analysis of Native and Denatured Protein R2. The first mass analyzer of a five-sector ZabSpec-T tandem mass spectrometer was used in all experiments (Micromass, Manchester, U.K.). This component corresponds to a ZabSpec triple-sector instrument of EBE geometry (E: electrostatic analyzer; B: magnet). The mass spectra were acquired using an Alpha station under the control of an OPUS 3.1 data system. Ion detection was achieved by using a photon multiplier located after the second electrostatic field.

The protein samples were dissolved either in a water/methanol/acetic acid mixture (50:50:1, "denaturing" conditions) or in an aqueous solution of 20 mM ammonium bicarbonate, pH 8.0. In both cases, the concentration of

enzyme was 25 μM. The protein solutions were introduced into the electrospray ion source by continuous infusion at a flow rate of 10 μL·min^{-1}, using a syringe pump (Harvard Apparatus, Model 11). The mass range *m*/*z* 6000−1000 was scanned at 20 s per decade. The accelerating voltage was 4000 V. Peptides originating from the tryptic digest of the nitrated protein were analyzed by electrospray at a concentration of approximately 5 μM in methanol. The mass scale *m*/*z* 4000−50 was scanned at 5 s per decade with a resolution of 1000 at 10% valley. Other experimental conditions were identical to those used for the protein analysis.

EPR Spectroscopy of Protein R2. Solutions of protein R2 were analyzed for Tyr122 free radical concentration at 77 K using a Varian E109 spectrometer, calibrated with the stable radical 1,1-dipheny-2-picrylhydrazyl (*21*). Experimental conditions were the following: microwave power 10 mW, microwave frequency 9.32 GHz, modulation amplitude 1 mT.

Measurement of R2 Activity. Experimental conditions were essentially as reported in ref *27*, using a 4-fold molar excess of the R1 subunit to complement for R2 activity. Thioredoxin and thioredoxin reductase, both from *E. coli*, were used as reducing agents. The reaction carried out at 25 °C and started by addition of 500 μM [5-^{3}H]CDP was linear with time over 5 min. Hydrolysis of phosphate groups and separation of radiolabeled cytidine from deoxycytidine by reverse-phase HPLC were performed as previously described (*21*).

RESULTS

Nitration of Peroxynitrite-Modified E. coli Protein R2 Analyzed by Spectrophotometry. In our previous work, formation of nitrotyrosine upon treatment of mouse and bacterial R2 proteins by peroxynitrite has been demonstrated by immunoblotting with an anti-nitrotyrosine antibody (*21*). Nitration was confirmed here by UV−visible spectroscopy using a recombinant R2 protein from *E. coli*. As already published (*28*), the native protein in water (pH 5.5) exhibited several absorption bands revealing the presence of a μ-oxo-bridged diferric iron center at 327 and 368 nm and a tyrosyl free radical at 392 and 410 nm (Figure 1, spectrum a). A new, wide peak with a maximum at 357 nm appeared in the samples incubated with 200 (spectrum b) or 400 μM (spectrum c) peroxynitrite. The intensity of the new absorption band increased with the peroxynitrite concentration. The spectrum of a protein incubated with decomposed peroxynitrite did not exhibit this increased absorbance at 350 nm (spectrum d in Figure 1 and spectrum b in the inset of Figure 1). Since the absorption maximum of authentic 3-nitrotyrosine at pH 5.5 is centered at 356 nm, the absorbance changes observed in peroxynitrite-modified protein R2 suggested nitration of some tyrosine residues. Interestingly, a significant loss of the absorbance at 410 nm was also observed in the spectra of the protein treated with peroxynitrite (inset of Figure 1, spectrum a). This is indicative of an effect on the tyrosine residue carrying the free radical. A much smaller decrease was sometimes observed in the sample incubated with decomposed peroxynitrite (inset of Figure 1, spectrum b). At alkaline pH, there is a red shift in the absorption maximum of 3-nitrotyrosine. When the pH of the solution was changed from 5.5 to 8.3, the new peak resulting from peroxynitrite treatment was effectively displaced from 357 to 422 nm (inset of Figure 1, spectrum c),

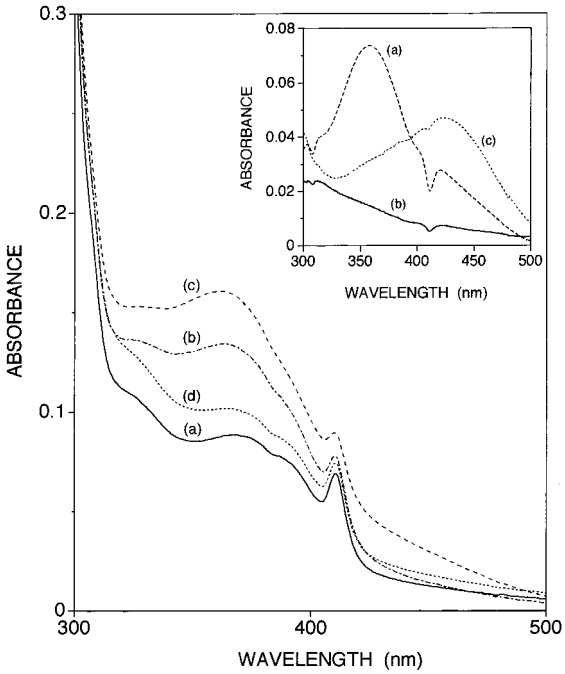

FIGURE 1: Absorbance spectra of peroxynitrite-modified *E. coli* protein R2. Protein R2, 5 μM, was reacted with peroxynitrite in 50 mM Tris·HCl buffer, pH 7.6. The sample was desalted, and the absorbance spectrum of a protein solution concentrated to 9 μM in water (pH 5.5) was recorded. Control (a); peroxynitrite, 200 μM (b); peroxynitrite, 400 μM (c); decomposed peroxynitrite, 400 μM (d). Inset: Difference spectra of peroxynitrite-modified protein R2 vs the untreated control. (a, b) Peroxynitrite, 400 μM, and decomposed peroxynitrite, 400 μM, respectively; spectra of 9 μM protein R2 recorded in water (pH 5.5). (c) Peroxynitrite, 400 μM; spectra of protein R2, 5 μM, recorded in 50 mM NH_4HCO_3 buffer, pH 8.3.

corresponding to the absorbance maximum of 3-nitrotyrosine at this pH. Under these conditions, quantification of the nitrotyrosine formed at a peroxynitrite concentration of 400 μM indicated a mean yield of 2.0 ± 0.3 nitrotyrosines per R2 dimer (mean ± SEM of 5 independent experiments).

Nitration of Peroxynitrite-Modified E. coli Protein R2 Analyzed by Mass Spectrometry. Effects of peroxynitrite on *E. coli* protein R2 were also investigated by electrospray-ionization mass spectrometry (ESI-MS). The mass spectrum of denaturated protein R2 shown in Figure 2 indicated a homogeneous sample with a measured mass of 43 392 Da, in agreement with the predicted mass of 43386 Da expected for the iron-free apoprotein R2. The deconvoluted mass spectrum displays additional broad peaks, due to the attachement of alkali metal ions and solvent molecules to the protein ions. Because of the weak intensity of the signal shown in Figure 2, it was not possible to assign reliably these ions, including one at 43 544 Da. The protein was further analyzed under nondenaturing solvent conditions (20 mM ammonium bicarbonate aqueous solution), allowing detection of peroxynitrite-mediated effects on the quaternary structure of R2 dimers. Despite the high molecular weight of the dimer, the *m*/*z* profile of the native, untreated protein was extremely well resolved (Figure 3A). The protein appeared essentially as a dimer containing two (Fe−O−Fe) cofactors. The mass of the dimer, measured by deconvolution of the electrospray spectrum, was 80 733 Da (Figure 3A, inset) compared to a calculated value of 87 028.8 Da. Formation of some nonspecific tetrameric species was also observed (*m*/*z* above

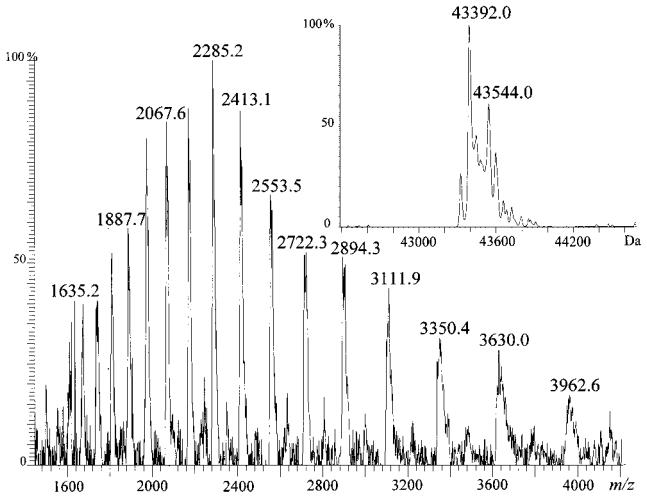

FIGURE 2: Electrospray mass spectrum of protein R2, recorded under denaturing solvent conditions (water/methanol/acetic acid 50:50:1). The inset displays the deconvoluted mass spectrum.

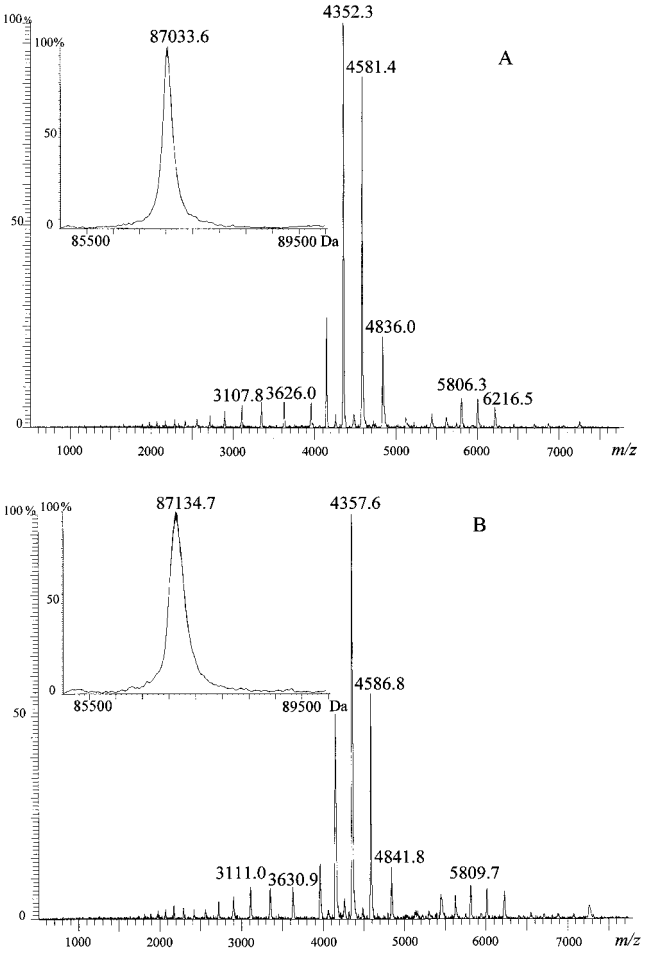

FIGURE 3: Electrospray mass spectra of native (A) and peroxynitrite-modified (B) protein R2 recorded under nondenaturing solvent conditions (20 mM ammonium bicarbonate aqueous solution). Peroxynitrite concentration was 400 μM. Insets display the deconvoluted mass spectra.

5500), as well as monomers still containing one metal center (*m*/*z* in the 2500−3600 range). The close agreement between the experimental mass and the predicted one allowed us to hope that small mass increments, such as those expected from tyrosine nitration(s), might be detected under these conditions. The measured mass of protein R2 reacted with 400 μM peroxynitrite was 87 134 Da (Figure 3B), corresponding to a mass increase of 101 Da compared to the control and of 105 Da with regard to the calculated value. Since nitration of a single tyrosyl amino acid would have resulted in a net mass increase of 45 Da, these results indicated approximately 2 nitrations per R2 dimer, in agreement with the data obtained by UV−Vis spectroscopy. Additionally, there was no evidence of an iron-free monomer or dimer in the mass spectrum of the peroxynitrite-treated protein, suggesting that the diiron metal cluster was not released upon R2 treatment with peroxynitrite. There was also no significant increase in the small amount of monomer detected, indicating that peroxynitrite treatment had not promoted the dissociation of R2 dimers. Noncovalent and unspecific aggregation that could have occurred in the gas phase during the electrospray analysis might have been responsible for an artifactual mass increase. Therefore, protein R2 incubated with 400 μM peroxynitrite was also analyzed under denaturing conditions to eliminate noncovalent adducts. The corresponding spectra revealed mass increases from 50 to 70 Da over the untreated control in three different experiments (data not shown). Further, the measured mass of a protein sample incubated with 400 μM decomposed peroxynitrite was 43 386 Da under denaturating conditions, identical to the theoretical mass of apoR2 (data not shown). It was concluded from these results that nitration of tyrosine residues was the predominant chemical modification induced in protein R2 by peroxynitrite. Both spectrophotometry and mass spectrometry analyses indicated a mean of 2 nitrotyrosines formed per R2 dimer at a peroxynitrite concentration of 400 μM.

Identification of the Nitrated Tyrosine Residues. To identify which tyrosine residues were nitrated, tryptic digests of protein R2 incubated with 100, 200, and 400 μM peroxynitrite were analyzed by reverse-phase HPLC with absorbance detection set at 350 nm for monitoring the nitrated peptides (Figure 4). After a first purification step using a C4 column, the fractions corresponding to each nitrated peptides were pooled and further purified on a C18 column. Only one peptide was eluted, showing that each peak in the C4 elution profile still corresponded to a single peptide, carrying a nitro group. In five experiments, nitration was always noted on three of the peptides. But in two out of the five experiments, one additional nitrated peptide was detected at the highest concentration of peroxynitrite tested (i.e., 400 μM), as shown in Figure 4. It corresponded to the N-terminal peptide AYTTFSQTK. The three peptides repeatedly nitrated were also sequenced. They were identified as fragments 58−70 (peptide P1), 121−127 (P2), and 285−292 (P3). The sequence of each of these peptides included only one tyrosine residue, which was Tyr62, Tyr122 (harboring the free radical), and Tyr289 in P1, P2, and P3, respectively (Table 1), as well as Tyr2 for the peptide inconsistently modified. This tyrosine amino acid did not appear in the sequence of the trypsin-digested nitrated peptides, suggesting that it had been changed to a nitrotyrosine by peroxynitrite. Unfortunately, under our experimental conditions, nitrotyrosine could not be directly detected, because it eluted at the same retention time as a byproduct of the sequencing reaction mixture. Finally, a mass increase of 45 Da was measured for the three peptides P1, P2, and P3 when analyzed by MS (Table 1). No other chemical modification could be detected on the other amino acids of the peptides sequenced, including

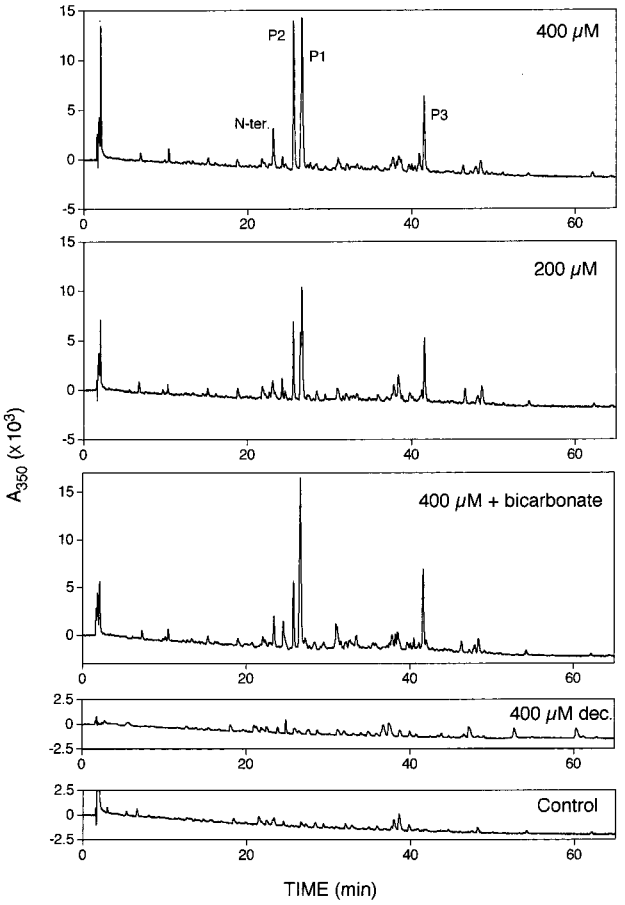

FIGURE 4: Reverse-phase HPLC profile of tryptic peptides from peroxynitrite-modified protein R2. Elution was performed as described under Experimental Procedures. From bottom to top: untreated control, protein R2 incubated for 5 min with 400 μM decomposed peroxynitrite, with 400 μM peroxynitrite in the presence of 25 mM sodium bicarbonate, with 200 μM and with 400 μM peroxynitrite without added bicarbonate. Nitrated peptides P1, P2, and P3 are indicated, as well as an N-terminal peptide (N-ter.) which was not present in every experiment. A shoulder in peak P1 corresponds to partial proteolytic cleavage of P1 with the two additional N-terminal amino acids Asp-Arg.

Table 1: Identification and Mass Determination of the Three Peptides Repeatedly Nitrated

peptide	sequence[a]	molecular mass[b] experimental	molecular mass[b] theoretical ($X = Y{-}NO_2$)
P1 (58−70)	DRID**X**QALPEHEK	1658.8	1658.8
P2 (121−127)	S**X**THIIR	934.4	934.5
P3 (285−292)	DWAD**X**LFR	1130.6	1130.5

[a] Nitrated peptides were identified by tryptic digestion of peroxynitrite-treated protein R2, followed by separation of peptides by reverse-phase HPLC and sequencing. In untreated controls, **X** is a tyrosine residue which was not detected in the peroxynitrite-treated samples. [b] The molecular mass of the purified peptides was determined by ESI-MS and compared to a calculated mass where *X* stands for a nitrotyrosine.

Trp286 in P3. It was therefore concluded that the tyrosine residues Tyr62, Tyr122, and Tyr289 were specifically nitrated by peroxynitrite in protein R2. Fragmentation of peptide P2 during ESI-MS analysis unambiguously confirmed the presence of a nitrotyrosine instead of a tyrosine residue at the Tyr122 position (Figure 5). Since the rate-limiting step in the nitration reaction is the one-electron

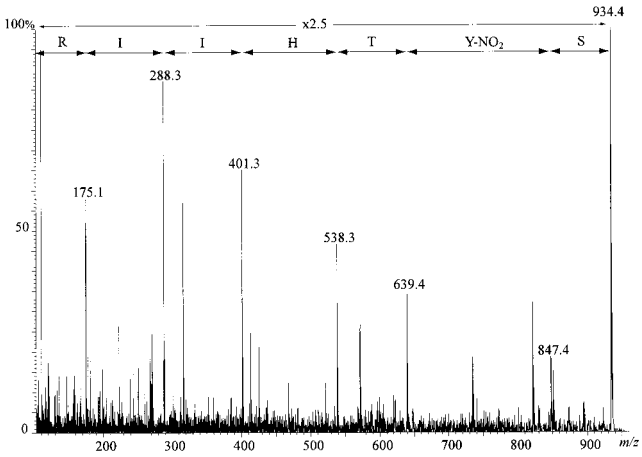

FIGURE 5: Electrospray mass spectrum of peptide P2 isolated by reversed-phase HPLC from the tryptic digest of protein R2 incubated with 400 μM peroxynitrite. The *m*/*z* values are indicated on the top of the diagnostic peaks belonging to the Y-type series according to the nomenclature of mass spectral fragmentations of peptides (*43*).

Table 2: Nitration of Specific Peptides in Protein R2 as a Function of Peroxynitrite Concentration

peroxynitrite[a] concn (μM)	nitrotyrosine per monomer[b]	nitrated Tyr in each peptide[c] (%) P1	P2	P3
100	0.70 ± 0.1	38 ± 10	14 ± 1	18 ± 1
200	0.85 ± 0.05	43 ± 2	22± 3	20 ± 3
400	1.1 ± 0.2	50 ± 4	36 ± 2	19 ± 0.5
400 + bicarbonate	1.1 ± 0.3	68 ± 5	15 ± 3	24 ± 1

[a] Peroxynitrite was added to 5 μM protein R2 in 50 mM Tris·HCl buffer, pH 7.6. When required, the buffer was supplemented with 25 mM sodium bicarbonate, pH 7.6. [b] The concentration of nitrotyrosine was quantified at 425 nm and pH 8.3 after protein desalting, as described in the Experimental Procedures. Values are the ratio of nitrotyrosine concentration to protein concentration. [c] After protease digestion, the nitrated peptides were separated by reverse-phase HPLC with absorbance detection set at 350 nm, as shown on Figure 4. The fraction of each nitrated peptide in the elution profile was determined after integration of the absorption peaks at 350 nm. The product of this value by the number of nitrotyrosine per monomer is the fraction of nitrated tyrosine in a peptide, expressed as the percentage of a given peptide recovered in a nitrated state. Data are mean ± SEM of two independent experiments.

oxidation of the tyrosine residue (*4*), it raised the question whether the radical character of Tyr122 might have significantly increased the nitration yield of this tyrosine residue, compared to the normal Tyr62 and Tyr289. As shown in Table 2, this was clearly not the case. At the lowest concentration of peroxynitrite, the nitration yield of Tyr122 was even lower than that of the two other tyrosine residues, especially Tyr62. In fact, it seemed that each nitrated tyrosine exhibited a different reactivity. Nitration of Tyr62 and Tyr289 was almost maximal at 100 μM peroxynitrite, while nitration of Tyr122 was weak at 100 μM but steadily increased with peroxynitrite concentration. Furthermore, Tyr62 was approximately twice more reactive than Tyr289.

Peroxynitrite breakdown is accelerated in the presence of bicarbonate, since $ONOO^-$ reacts rapidly with CO_2 (*4*). The adduct thus formed exhibits a reactivity different than that of $ONOO^-$/ONOOH. In particular, nitration of aromatics has been shown to be enhanced in the presence of CO_2 (*4*). Bicarbonate is a contaminant in buffers equilibrated with air and, owing to the catalytic role of CO_2 in the reaction with

peroxynitrite, might have significantly influenced the nitration of protein R2 in the experiments described here. Also, bicarbonate is present at higher concentrations (10−30 mM) in tissues, suggesting that the reaction of $ONOO^-$ with CO_2 might play a predominant role *in vivo*. To better understand how protein R2 could be nitrated under physiological conditions, we investigated the effect of peroxynitrite in the presence of 25 mM bicarbonate. Unexpectedly, at a concentration of 400 μM peroxynitrite, the mean number of nitrotyrosines per monomer did not change (Table 2). But the specificity of the nitration reaction was considerably modified (Figure 4 and Table 2). Nitration of the radical-carrying Tyr122 was decreased by more than 50%, whereas the two other tyrosine residues, and especially Tyr62, became more susceptible to nitration.

All these experiments were performed in Tris·HCl buffer. It has been reported that Tris can react with peroxynitrite (*10*), raising the possibility that this buffer could have modified peroxynitrite reactivity toward protein R2. Therefore, in one experiment, the buffer was changed to phosphate, 100 mM, pH 7.6. Nitration of protein R2 by 400 μM peroxynitrite increased from 1.1 to 2.0 nitrotyrosines/monomer, but the specificity of the nitration was not considerably modified. We only noticed a relative small increase in the nitration of Tyr289 (+30%) and a corresponding decrease in the modification of Tyr122. Similar results were obtained with 250 μM peroxynitrite (data not shown).

Effect of Peroxynitrite on the Activity of E. coli Protein R2. The free radical located on Tyr122 is involved in catalysis through a long-range hydrogen atom transfer pathway between Tyr122 on protein R2 and Cys439 on protein R1 (*29*). We have already observed that peroxynitrite induced a partial loss of the free radical (Figure 1), in addition to the nitration of the tyrosyl amino acid carrying the radical. We therefore questioned whether there was a link between these two events, and to what extent these changes inhibited the activity of the protein. In one experiment, we monitored in parallel the nitration of peptides P1, P2, and P3, the variation in the concentration of the free radical, and the decrease in R2 activity induced by different concentrations of peroxynitrite. As shown in Figure 6, the dose-dependent decrease in the free radical concentration and the decrease in unmodified (not nitrated) Tyr122 were almost superimposable, strongly suggesting that the observed loss of the free radical was exclusively caused by nitration of Tyr122. In contrast, the decrease in R2 activity was much more pronounced than the changes affecting Tyr122 for all the peroxynitrite concentrations tested. It was concluded that inactivation of protein R2 was not only caused by the destruction of the free radical at Tyr122. A sample incubated with 400 μM decomposed peroxynitrite exhibited less than a 10% decrease in free radical concentration, less than 10% of nitrated Tyr122, and no significant variation in R2 activity compared to the untreated control.

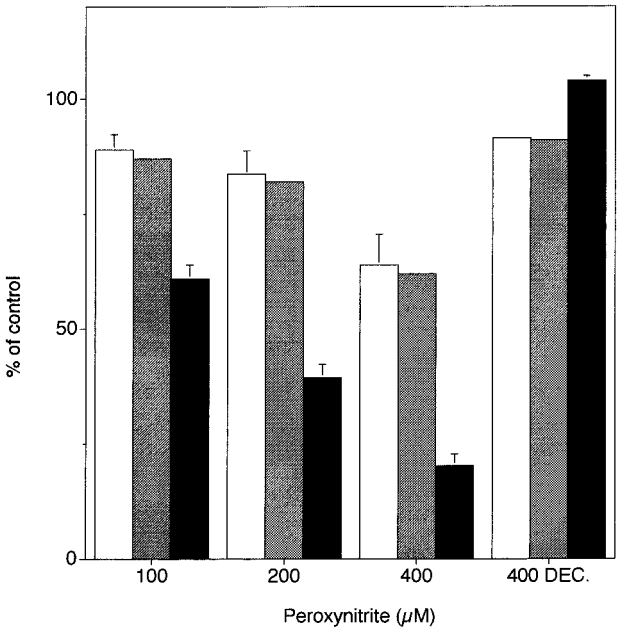

FIGURE 6: Comparison of Tyr122 nitration with tyrosyl free radical destruction and inactivation of *E. coli* protein R2 induced by peroxynitrite. Protein R2 (5 μM) was reacted with 100, 200, or 400 μM peroxynitrite or with 400 μM decomposed peroxynitrite (400 DEC.), in 50 mM Tris·HCl buffer, pH 7.6. Variations in the tyrosyl free radical concentration (white bars) were estimated from the changes in the absorbance of the radical at 410 nm, relative to the control (other values obtained from the variations in the amplitude of the free radical EPR signal did not differ by more than 14% with the data presented). The amount of nitrotyrosine 122 calculated as described under Table 2 was used to calculate by difference the fraction of intact, non-nitrated Tyr122 (gray bar). The enzymatic activity of protein R2 (black bars) was measured in the presence of a 4-fold molar excess of protein R1. Results are means ± SD of three determinations.

DISCUSSION

Previously we demonstrated that peroxynitrite inactivated the mouse R2 subunit of ribonucleotide reductase and induced the nitration of tyrosine residues in the murine and the bacterial protein (*21*). In the present study, we have identified the modified tyrosine amino acids in the *E. coli* subunit by combining ESI-MS and peptide sequencing. We have also investigated the relationship between tyrosine nitration and inactivation of the protein by peroxynitrite. The excellent behavior of protein R2 from *E. coli* when analyzed by ESI-MS under nondenaturing conditions allowed the recovery of a native, dimeric, iron-containing protein with a very good yield. Interestingly, the quaternary structure of a peroxynitrite-modified protein R2 was not significantly altered. In particular, the Fe−O−Fe cofactor was not released after peroxynitrite treatment, since there was no evidence of apoR2 formation in the corresponding ESI-MS spectrum. This stability was interpreted as a first indication of a selective effect of peroxynitrite on protein R2. Using two independent techniques, namely, UV−visible spectroscopy and ESI-MS, a mean number of 2 tyrosines/dimer were shown to be nitrated by 400 μM peroxynitrite. After protease digestion, peptide sequencing, and mass analysis of the nitrated peptides, nitration was found to target repeatedly only 3 among the 16 tyrosine amino acids present in protein R2 from *E. coli*. Occasionally, Tyr2 in the N-terminus of the protein was also nitrated but to a smaller extent. Among these three nitrated tyrosines, two were localized at the surface of the protein (Tyr62 and Tyr289), as shown in Figure 7. The last one is Tyr122, which is in a one-electron-oxidized free radical state, buried deep inside the protein core close to the diferric center (*29*). The existence of a free radical-bearing tyrosine residue in protein R2 offers the unique opportunity to compare the nitrating efficiency of

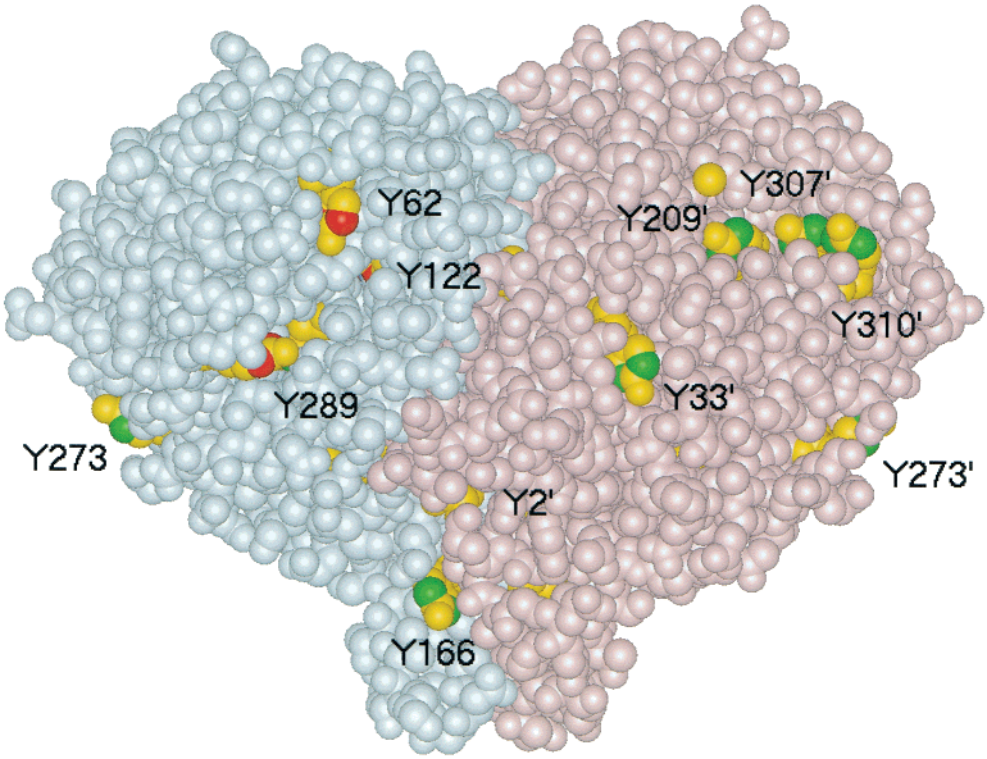

FIGURE 7: Location of the nitrated tyrosine residues in the *E. coli* R2 protein. The dimeric R2 subunit of ribonucleotide reductase is shown in a space-filling model using the 3D structure coordinates of metR2 previously published (*29*). The alpha chain is colored pale blue, and tyrosine residues are yellow. Epsilon carbon atoms in tyrosine residues susceptible, or not, to nitration by peroxynitrite are respectively colored red and green. The figure was created by the program WebLab ViewerPro from MSI.

peroxynitrite toward normal vs one-electron-oxidized tyrosine residues. It has been suggested that tyrosine nitration by nitrosoperoxycarbonate, $ONOOCO_2^-$, a reaction product of $ONOO^-$ with CO_2, might proceed via a radical mechanism (*4*), which might involve a reactive species with a $^\bullet NO_2$ character. CO_2 is normally present as a contaminant in biological buffers equilibrated with air. Therefore, not only the $ONOO^-$/ONOOH couple but also $ONOOCO_2^-$ should be a relevant effector in our experiments, even in those without added bicarbonate. Reactions between two radicals are usually extremely fast [for instance, $k = 3 \times 10^9\ M^{-1}\cdot s^{-1}$ for the association of $^\bullet NO_2$ with a tyrosyl free radical (*2*)]. The rate-limiting step in tyrosine nitration by free $^\bullet NO_2$ is the oxidation of tyrosine. Therefore, it could seem surprising at first glance that the efficiency of Tyr122 nitration would not be higher than nitration of Tyr62 and Tyr289. Additionnally, the close proximity of a metal center near Tyr122 was expected to further increase the nitration yield of this amino acid, as previously described for other metalloproteins (*8, 10, 30*). Obviously, there are some important factors that are limiting the reactivity of peroxynitrite toward Tyr122. One of these is likely to be the restricted accessibility of the buried tyrosine, belonging to an α helix in the hydrophobic core of protein R2. Previous studies aimed to delineate the structural basis for an efficient reduction of the free radical by radical scavengers have indicated that negatively charged molecules do not gain access to the radical/metal center of protein R2 from *E. coli* (*23, 31*). Therefore, only the uncharged peroxynitrous acid, but not the two anions $ONOO^-$ and $ONOOCO_2^-$, should have the ability to react with Tyr122. Assuming that, in the absence of added bicarbonate, our buffer at pH 7.6 was contaminated with the usual levels of CO_2 [approximately 0.01 mM at 25 °C (*4*)] and considering that the fast, catalytic reaction of $ONOO^-$ with CO_2 is not favorable to the formation of ONOOH (*4*), we can explain the reduced efficiency of Tyr122 nitration by the relatively small amount of ONOOH that should be formed in the incubation medium. This interpretation is supported by results from experiments performed in the presence of 25 mM bicarbonate. Nitration of Tyr122 was reduced by more than 50%, suggesting that formation of $ONOOCO_2^-$ occurred at the expense of the species reacting with Tyr122, probably ONOOH. However, under conditions of high bicarbonate concentrations which dramatically reduce the formation of ONOOH, we cannot rule out the involvement of other nitrating agents. The free radical $^\bullet CO_2$ formed in the process of $ONOOCO_2^-$ decay might be a candidate.

The two other tyrosine residues Tyr62 and Tyr289 belong to the α1 and αG helices, respectively, which are both situated on the outsite of the R2 eight-helix barrel (*29*). Tyrosine is nitrated by peroxynitrite at the 3 position of the aromatic ring. In the crystal structure of *E. coli* protein R2, at least one of the two epsilon carbons of the two susceptible residues is clearly facing the outside solvent, apparently far enough from other atoms to accommodate a nitro group (Figure 7). The nitration of Tyr62 and Tyr289 is thus in agreement with the good accessibility of these two residues. The amino acid sequence beside a nitrated tyrosine has been proposed to influence significantly the effectiveness of the nitration reaction (*10*). From our data, there is no doubt that important parameters other than accessibility contribute to the specificity of tyrosine nitration. For instance, Tyr289 is about half as reactive as Tyr62, a difference that cannot be compensated by increasing peroxynitrite concentration. Addition of bicarbonate to promote formation of the potent nitrating agent nitrosoperoxycarbonate increased nitration of

these two tyrosine residues but still spared the other ones. For instance, Tyr33, Tyr273, and Tyr310, although surface-exposed, were not nitrated to a significant extent (Figure 7). Careful examination of the amino acids surrounding Tyr62 and Tyr289 did not reveal any particular differences, relative to the unreactive tyrosine residues. It is doubtful that the diferric iron played a role in the nitration process as the distance to the closest iron atom was 21.9 Å in both cases, whereas it was only 8.6 and 14.9 Å for Tyr 209 and Tyr307, respectively. Thus, in this model, the molecular basis for the selectivity of the nitration remains unclear.

Nitration of Tyr122 neutralized the free radical located on this residue, as indicated by the very close correlation between the loss of tyrosyl free radical EPR signal and the decrease in unmodified Tyr122. Since the free radical is required for activity, the resulting inactivation of protein R2 caused by free radical destruction was expected, and observed. However, inhibition of *E. coli* R2 activity was much more pronounced than nitration of Tyr122. These findings are in contrast to the results of a previous study, which showed a very good parallelism between mouse R2 inactivation and loss of the tyrosyl free radical (*21*). Since nitration of the murine protein is also less intense, it seems that peroxynitrite-induced nitration is more specifically directed against the free radical-carrying residue in the mouse, compared with *E. coli*. In agreement with this hypothesis, we observed that Tyr62 and Tyr289 are not conserved in the mouse R2 protein (*29*). Thus, nitration of Tyr62 or Tyr289 might play a critical role in the inactivation of protein R2 from *E. coli*. Ile60 and Ala64, close to Tyr62, have been proposed to participate with a few other hydrophobic residues to the binding of the complementary subunit R1 (*29*). If nitration of Tyr62 results in a decreased affinity of R2 for R1, it would also contribute to inhibit activity. Moreover, we cannot exclude the occurrence of peroxynitrite-induced modifications other than tyrosine nitration (*5*, *21*).

In vivo, nitric oxide can exert both pro- and antitumor effects (*32*−*36*). This dual role of NO in cancer has been suggested to be dose-dependent (*32*, *33*), higher concentrations of NO causing tumor cytostasis, cytotoxicity, and apoptosis. In particular, Fidler and co-workers have conclusively shown that potent expression of iNOS *in vivo* inhibited tumorigenicity and metastasis in animal cancer models (*34*−*36*). An elevated iNOS activity has been also detected in some human tumor tissue (*16*, *37*). Several reports from our group (*17*, *19*, *38*) and others (*18*, *39*) support a significant role of ribonucleotide reductase inhibition in iNOS-mediated cytostasis. Contrasting with our previous results in a cell culture model (*21*), positive immunostaining for 3-nitrotyrosine was often associated with iNOS expression in animal and human tumors (*13*, *40*−*42*), suggesting peroxynitrite production within iNOS-expressing tumors in vivo. The present study suggests that ribonucleotide reductase might be a potential target for peroxynitrite. Irreversible inactivation of the enzyme by nitration might contribute to the antitumor action of iNOS in vivo.

ACKNOWLEDGMENT

We thank Pr. M. Fontecave for providing recombinant materials, and B. Wolfersberger and R. Auger for excellent technical assistance.

REFERENCES

1. Beckman, J. S., and Koppenol, W. H. (1996) *Am. J. Physiol. 271*, C1424.
2. Ischiropoulos, H. (1998) *Arch. Biochem. Biophys. 356*, 1.
3. Halliwell, B. (1997) *FEBS Lett. 411*, 157.
4. Squadrito, G. L., and Pryor, W. A. (1998) *Free Radical Biol. Med. 25*, 392.
5. Ischiropoulos, H., and Al-Mehdi, A. B. (1995) *FEBS Lett. 364*, 279.
6. Berlett, B. S., Levine, R. L., and Stadtman, E. R. (1998) *Proc. Natl. Acad. Sci. U.S.A. 95*, 2784.
7. Hühmer, A. F. R., Gerber, N. C., Demontellano, P. R. O., and Schoneich, C. (1996) *Chem. Res. Toxicol. 9*, 484.
8. Yamakura, F., Taka, H., Fujimura, T., and Murayama, K. (1998) *J. Biol. Chem. 273*, 14085.
9. Smith, C., Carson, M., van der Woerd, M., Chen, J., Ischiropoulos, H., and Beckman, J. S. (1992) *Arch. Biochem. Biophys. 299*, 350.
10. Crow, J. P., Ye, Y. Z., Strong, M., Kirk, M., Barnes, S., and Beckman, J. S. (1997) *J. Neurochem. 69*, 1945.
11. Roberts, E. S., Lin, H. L., Crowley, J. R., Vuletich, J. L., Osawa, Y., and Hollenberg, P. F. (1998) *Chem. Res. Toxicol. 11*, 1067.
12. Jordan, A., and Reichard, P. (1998) *Annu. Rev. Biochem. 67*, 71.
13. Ambs, S., Merriam, W. G., Bennett, W. P., Felley-Bosco, E., Ogunfusika, M. O., Oser, S. M., Klein, S., Shields, P. G., Billiar, T. R., and Harris, C. C. (1998) *Cancer Res. 58*, 334.
14. Gal, A., Tamir, S., Kennedy, L. J., Tannenbaum, S. R., and Wogan, G. N. (1997) *Cancer Res. 57*, 1823.
15. Weninger, W., Rendl, M., Pammer, J., Mildner, M., Tschugguel, W., Schneeberger, C., Sturzl, M., and Tschachler, E. (1998) *Lab. Invest. 78*, 949.
16. Liu, C. Y., Wang, C. H., Chen, T. C., Lin, H. C., Yu, C. T., and Kuo, H. P. (1998) *Br. J. Cancer 78*, 534.
17. Lepoivre, M., Chenais, B., Yapo, A., Lemaire, G., Thelander, L., and Tenu, J.-P. (1990) *J. Biol. Chem. 265*, 14143.
18. Kwon, N. S., Stuehr, D. J., and Nathan, C. F. (1991) *J. Exp. Med. 174*, 761.
19. Lepoivre, M., Flaman, J. M., Bobe, P., Lemaire, G., and Henry, Y. (1994) *J. Biol. Chem. 269*, 21891.
20. Roy, B., Lepoivre, M., Henry, Y., and Fontecave, M. (1995) *Biochemistry 34*, 5411.
21. Guittet, O., Ducastel, B., Salem, J. S., Henry, Y., Rubin, H., Lemaire, G., and Lepoivre, M. (1998) *J. Biol. Chem. 273*, 22136.
22. Gaudu, P., Niviere, V., Petillot, Y., Kauppi, B., and Fontecave, M. (1996) *FEBS Lett. 387*, 137.
23. Gerez, C., Elleingand, E., Kauppi, B., Eklund, H., and Fontecave, M. (1997) *Eur. J. Biochem. 249*, 401.
24. Sjöberg, B.-M., Hahne, S., Karlsson, M., Jörnvall, H., Göransson, M., and Uhlin, B. E. (1986) *J. Biol. Chem. 261*, 5658.
25. Crow, J., Beckman, J. S., and McCord, J. M. (1995) *Biochemistry 34*, 3544.
26. Gow, A., Duran, D., Thom, S. R., and Ischiropoulos, H. (1996) *Arch. Biochem. Biophys. 333*, 42.
27. Persson, A. L., Eriksson, M., Katterle, B., Potsch, S., Sahlin, M., and Sjoberg, B. M. (1997) *J. Biol. Chem. 272*, 31533.
28. Petersson, L., Gräslund, A., Ehrenberg, A., Sjöberg, B. M., and P., R. (1980) *J. Biol. Chem. 255*, 6706.
29. Nordlund, P., and Eklund, H. (1993) *J. Mol. Biol. 232*, 123.
30. Ischiropoulos, H., Zhu, L., Chen, J., Tsai, M., Martin, J. C., Smith, C. D., and Beckman, J. S. (1992) *Arch. Biochem. Biophys. 298*, 431.
31. Sahlin, M., Gräslund, A., Petersson, L., Ehrenberg, A., and Sjöberg, B.-M. (1989) *Biochemistry 28*, 2618.
32. Thomsen, L. L., and Miles, D. W. (1998) *Cancer Metastasis Rev. 17*, 107.
33. Jenkins, D. C., Charles, I. G., Thomsen, L. L., Moss, D. W., Holmes, L. S., Baylis, S. A., Rhodes, P., Westmore, K., Emson, P. C., and Moncada, S. (1995) *Proc. Natl. Acad. Sci. U.S.A. 92*, 4392.
34. Xu, L., Xie, K. P., and Fidler, I. J. (1998) *Hum. Gene Ther. 9*, 2699.

35. Juang, S. H., Xie, K. P., Xu, L., Shi, Q., Wang, Y. F., Yoneda, J. Y., and Fidler, I. J. (1998) *Hum. Gene Ther. 9*, 845.
36. Xie, K. P., Huang, S. Y., Dong, Z. Y., Gutman, M., and Fidler, I. J. (1995) *Cancer Res. 55*, 3123.
37. Klotz, T., Bloch, W., Volberg, C., Engelmann, U., and Addicks, K. (1998) *Cancer 82*, 1897.
38. Lepoivre, M., Flaman, J.-M., and Henry, Y. (1992) *J. Biol. Chem. 267*, 22994.
39. Wang, Z. Q., Wang, M. F., and Carr, B. I. (1998) *Hepatology 28*, 430.
40. Robertson, F. M., Long, B. W., Tober, K. L., Ross, M. S., and Oberyszyn, T. M. (1996) *Carcinogenesis 17*, 2053.
41. Kojima, M., Morisaki, T., Tsukahara, Y., Uchiyama, A., Matsunari, Y., Mibu, R., and Tanaka, M. (1999) *J. Surg. Oncol. 70*, 222.
42. Vickers, S. M., MacMillan-Crow, L. A., Green, M., Ellis, C., and Thompson, J. A. (1999) *Arch. Surg. 134*, 245.
43. Bieman, K. (1990) *Methods Enzymol. 193*, 886.

BI992206M